International Journal of Environment and Waste Management

ISSN online: 1478-9868 - ISSN print: 1478-9876
https://www.inderscience.com/ijewm

Statistical analysis and mathematical modelling of Plackett-Burman screening design to improve the fuel properties of oil palm fibre by torrefaction process

Chokchai Mueanmas, Panadda Indum

DOI: 10.1504/IJEWM.2023.10050952

Article History:

Received:	17 August 2021
Accepted:	06 July 2022
Published online:	30 December 2024

Statistical analysis and mathematical modelling of Plackett-Burman screening design to improve the fuel properties of oil palm fibre by torrefaction process

Chokchai Mueanmas* and Panadda Indum

Energy Engineering Program,
Faculty of Engineering,
Thaksin University,
Phatthalung 93210, Thailand
Email: chokchai@tsu.ac.th
Email: panadda_02419@hotmail.com
*Corresponding author

Abstract: In this study, the two-level Plackett-Burman design (PBD) was applied to screen the significant variables of torrefaction process of oil palm fibre (OPF). The independent parameters such as temperature, time, oxygen feed, heat rate and OPF size were studied. The %mass yield (%MY) and fuel properties including %moisture content (%MC), %volatile content (%VC), %ash content (%AC), %fixed carbon content (%FC) and heating value (HV) were selected as response variable. The results indicated that temperature, time, oxygen feed rate and heat rate performed statistically significant to the response of torrefied OPF. All obtained mathematical models showed a good fit with high coefficient of determination and their reliability was demonstrated by diagnostics plot. At the maximum experimental result, the %FC and HV of torrefied OPF increased by 13,483% and 27.42%, while the value of %MC and %VC decreased by 93.71% and 42.55%, respectively, as compared with the raw OPF. Thus, the torrefaction seems to be a potential process to improve the quality of fuel properties of OPF.

Keywords: oil palm fibre; OPF; torrefaction; Plackett-Burman screening design; proximate analysis; heating value.

Reference to this paper should be made as follows: Mueanmas, C. and Indum, P. (2025) 'Statistical analysis and mathematical modelling of Plackett-Burman screening design to improve the fuel properties of oil palm fibre by torrefaction process', *Int. J. Environment and Waste Management*, Vol. 36, No. 1, pp.14–32.

Biographical notes: Chokchai Mueanmas received his Bachelor's in Industrial Chemistry from Prince of Songkla University, Pattani, Thailand in 2004, and Doctoral in Chemical Engineering from Prince of Songkla University, Songkhla, Thailand in 2011. He is currently working as an Assistant Professor in the Energy Engineering Program at Faculty of Engineering, Thaksin University, Phatthalung, Thailand.

Panadda Indum received her Bachelor's in Chemistry from Prince of Songkla University, Songkhla, Thailand in 2016, and Master's in Energy Engineering from Thaksin University, Phatthalung, Thailand in 2019. She is currently working as an academician position at Faculty of Technology Community Development, Thaksin University, Phatthalung, Thailand.

1 Introduction

Biomass has great potential as a renewable energy resource to replace fossil fuel. Its property of zero carbon emission can help to reduce carbon dioxide emissions, environmental problems and resource depletion. Biomass is easily obtained and is characterised by a short life cycle. To reduce the impact on food crops, interest has turned to the potential of residual biomass as a bioresource. Oil palm fibre (OPF) is a waste material from the production of palm oil. Around 0.19 ton of OPF is produced per ton of oil palm fresh fruit bunch (Energy, 2019). An estimated total of 2.13 million tons of OPF were discarded in 2016 (Petchseechoung, 2017) which could have been used as solid fuel for power generation or industrial purposes. However, OPF is not suitable for transportation and storage since it is characterised by low energy density, biodegradation, strong hydrophilicity, hygroscopic behaviour and poor grindability. In addition, raw OPF has a high %MC and %VC with low %FC and heating value (HV) which affect the combustion efficiency of the material. Therefore, it cannot be directly utilised for thermochemical conversion. To improve the fuel properties of OPF, it has to be pretreated before being processed.

Torrefaction is the most effective way to improve the fuel properties of OPF. It is a mild pyrolysis or thermochemical process in which raw material is thermally degraded at temperatures of 200 to 300°C under 1 atm in the absence of oxygen (Su et al., 2018; Campbell et al., 2019). After processing, torrefied biomass shows improved physical, chemical and biochemical properties (Cheng et al., 2019). Gan et al. (2019) studied the torrefaction of de-oiled Jatropha seed kernel and found that the optimal condition of torrefaction, at 300°C and 60 min with a particle size of 0.5 to 1.0 mm, increased higher HV from 23.08 to 28.69 MJ/kg. Chen et al. (2018) evaluated the hygroscopic transformation of torrefied poplar and fir. The results indicated that hygroscopicity was reduced by up to 57.39% at 230°C. Singh et al. (2019) torrefied pigeon pea stalk (*Cajanus cajan*) to investigate the effect of temperature and residence time on physicochemical properties of the product. Their characterisation of torrefied pigeon pea stalk showed that the of oxygen/carbon and hydrogen/carbon ratios decreased when torrefaction temperature was increased. At a temperature of 275°C and residence time of 45 min, higher HV increased 28.6% due to the increased energy density and Hausner Ratio, moisture reabsorption, decreased bulk density and Carr compressibility index. Wang et al. (2018) explored the torrefaction of Norway spruce stem wood, stump and bark at temperatures ranging from 225 to 300°C with 30 and 60 min residence times. The results showed that this process could improve the physicochemical properties and grindability of the raw material. After torrefaction, hemicellulose and cellulose contents were lower, which reduced the fibrous structure. Also, the grindability was improved in the torrefied product. Many researchers have reported significant parameters for the torrefaction process of several materials. Lee et al. (2012) found that temperature and time were significant in the torrefaction of mixed softwoods. Chiou et al. (2015) examined the torrefaction of apple, grape, olive and tomato pomaces. The results showed that temperature had a greater effect than time on the mass and energy yields. Nam and Capareda (2015) investigated the parameters affecting the torrefaction of rice straw and cotton stalk. Based on statistical results, temperature was the main affecting parameter for rice straw, while the interaction of temperature and time was the most significant for cotton stalk. Other affecting parameters studied included heating rate (Talero et al., 2019;

Xu et al., 2019), particle size (Gan et al., 2019; Rasid et al., 2019) and oxidative condition (Uemura et al., 2013, 2015; Zhang et al., 2019).

The purpose of this study was to screen the effects on torrefaction of five factors: temperature, time, %oxygen feed, heat rate and OPF size. PBD was applied to the experimental design. The factors were evaluated from their effects on six responses: %MY, %MC, %VC, %AC, %FC and HV. The experimental results were fitted with the first-order model. Also, the adequacy of the mathematical model was verified by analysis of variance (ANOVA). The uniformity of the error distribution was checked by diagnostic plots. Finally, parameters with a confidence level greater than 95% (p-value < 0.05) for at least 1 response, were considered to have a significant effect on the torrefaction process of OPF.

2 Material and methodology

2.1 Materials

OPF was from the Palmdeesrinakorn Co., Ltd., in the Nakorn Sri Thammarat province of Thailand. The received sample was already processed to sizes between 2 and 10 cm. The fuel properties of the received OPF, determined by proximate analysis and HV, were as follows: MC, 10.49%; VC, 85.62%; AC, 3.59%; FC, 0.30% and HV, 4161 cal/g.

Figure 1 Schematic diagram of the experimental setup (see online version for colours)

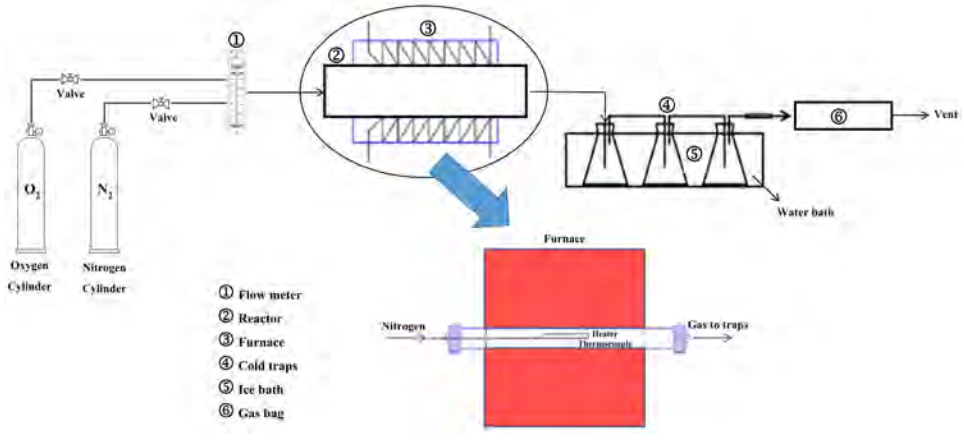

2.2 Materials

The OPF was torrefied in an iron tubular batch reactor measuring 50 cm length with a 5 cm internal diameter. The experiments were conducted in an electrical heating tube furnace as shown in Figure 1. Before each experiment, the reactor was purged with nitrogen for 10 min to remove undesired air/oxygen. An OPF quantity of 100 g was fed into the reactor and the independent parameters were set based on the PBD experimental

design shown in Table 2. The obtained product of each torrefaction was characterised by HV and proximate analysis.

2.3 Design of experiments

Plackett-Burman design (PBD) was employed to screen the factors that significantly affect the fuel properties of OPF. The independent factors of temperature (X_1), time (X_2), oxygen feed ratio (X_3), heat rate (X_4) and OPF size (X_5) were studies in the ranges shown in Table 1. Each independent variable was evaluated at two levels, –1 for low level and +1 for high level.

Table 1 Coded and actual level of independent variables used in the PBD experimental design

Symbol	*Variable*	*Unit*	*Coded variable level*	
			–1	*+1*
X_1	Temperature	°C	200	320
X_2	Time	minute	5	50
X_3	Oxygen feed	%	0	20
X_4	Heat rate	°C/min	5	30
X_5	OPF size	centimetre	2	10

The design space of the 12 experiments for the five factors was determined using Design-Expert® software 7.0.0 (trial version). All the experiments were performed at random, as shown in Table 2. Regression analysis was performed on the experimental data from the PBD, and the first-order linear model was established as equation (1),

$$Y = \beta_0 + \sum_{i=1}^{k} \beta_i X_i \tag{1}$$

where Y stands for the response, β_0 is the independent coefficient, β_i is the coefficient associated to each factor X_i. ANOVA was performed at 95% confidence level to determine the significant effect of each factor with regarding to the process. The F-values, p-values and R^2 were evaluated to check the efficiency of the model. The F-values, p-values and R^2 were evaluated to check the efficiency of the model. The variance of data was described by the F-value: if higher than the critical value, the parameters were more exact. A p-value less than 0.05 indicated the model terms were significant. Finally, the normal probability plots of the residuals, predicted versus actual plots, and the plots of the residuals versus the predicted response and run number were checked to establish the adequacy of the experimental data.

2.4 Fuel property analysis

Analysis of biomass fuel is necessary to assess its quality. The simplest and most common technique is HV and proximate analysis. The HV was determined using an automatic bomb calorimeter (LECO AC 500). The proximate analysis determined moisture, volatile matter, ash and fixed carbon.

Table 2 PBD of experiments for the study of five independence variable with experimental and predicted values

Run	*Actual level of variable*					*% MY*		*% MC*		*% VC*		*% AC*		*% FC*		*HV (Cal/g)*	
	X_1	X_2	X_3	X_4	X_5	*Actual*	*Predictive*	*Actual*	*Predictive*	*Actual*	*Predictive*	*Actual*	*Predictive*	*Actual*	*Predictive*	*Actual*	*Predictive*
1	320	50	0	5	2	35.75	36.39	0.69	0.71	49.19	50.54	9.36	9.50	40.75	39.25	4,664	4,795
2	320	50	0	30	10	40.33	40.31	0.90	0.93	52.02	51.31	8.04	8.11	39.04	39.65	4,736	4,901
3	200	50	20	5	10	81.00	81.88	0.96	0.89	71.84	74.28	4.44	4.91	22.76	19.93	4,481	4,428
4	200	50	20	30	2	86.33	86.70	0.86	0.92	71.46	71.87	4.22	4.08	23.45	23.13	4,500	4,468
5	320	5	20	30	2	54.36	54.43	1.10	1.01	60.65	61.70	5.78	6.08	32.47	31.21	5,302	5,158
6	200	5	0	5	2	91.67	90.56	0.66	0.61	83.96	81.46	4.24	4.65	11.14	13.28	4,479	4,487
7	320	5	20	30	10	54.33	53.98	1.09	1.11	64.40	63.29	5.65	5.80	28.86	29.80	5,089	5,191
8	320	50	20	5	2	40.00	39.12	0.87	0.89	54.22	52.14	9.04	8.61	35.88	38.35	4,935	4,894
9	320	5	0	5	10	46.33	46.89	0.80	0.80	60.99	62.50	8.02	7.79	30.18	28.90	5,232	5,019
10	200	50	0	30	10	84.50	83.52	0.89	0.84	73.26	71.86	4.79	4.68	21.06	22.62	4,572	4,403
11	200	5	0	30	2	94.00	94.92	0.70	0.74	78.86	80.64	3.81	3.54	16.63	15.08	4,483	4,561
12	200	5	20	5	10	92.90	92.83	0.81	0.88	85.37	84.65	3.83	3.48	9.99	10.98	4,450	4,619

2.4.1 Determination of moisture content

The moisture content of OPF was determined by drying the OPF at 100 ± 5°C in an electrical oven and calculating the weight loss. The procedure continued until constant weight loss was achieved. Moisture content was calculated from equation (2).

$$Moisture\ content(\%) = \frac{m_2}{m_1} \times 100 \tag{2}$$

where m_1 is the weight of OPF (g), m_2 is the weight of OPF after heating at 100 ± 5°C (g).

2.4.2 Determination of volatile content

The dried OPF was placed in a covered crucible and kept in an electric furnace at 900 ± 20°C for 10 min. The crucible was allowed to cool in a desiccator. The weight lost was reported as volatile matter, calculated from equation (3).

$$Volatile\ content(\%) = \frac{m_3}{m_2} \times 100 \tag{3}$$

where m_3 is the weight of OPF after heating at 900 ± 20°C (g)

2.4.3 Determination of ash content

The residual OPF after determination of volatile content was heated uncovered in an electric furnace at 700 ± 50°C for one and a half hours. The crucible was allowed to cool in a desiccator. This procedure was repeated until a constant weight was obtained. The residual OPF was reported as ash, calculated as follows:

$$Ash\ content(\%) = \frac{m_4}{m_3} \times 100 \tag{4}$$

where m_4 is the weight of OPF after heating at 700 ± 50°C (g).

2.4.4 Determination of fixed carbon content

The fixed carbon was determined as follows:

$$Fixed\ carbon\ content\ (\%) = 100 - \%\ moisture - \%\ volatile\ matter - \%\ ash \tag{5}$$

3 Results and discussion

3.1 ANOVA and estimated regression of each response

The improvement in fuel properties due to the torrefaction of OPF can be seen in the results of the 12 numerical runs (Table 2). The magnitude of responses for %MY ranged from 35.75 to 94.00%, %MC ranged from 0.69 to 1.10%, %VC ranged from 49.19 to 85.37%, %AC ranged from 3.81 to 9.36%, %FC ranged from 9.99 to 40.75 and HV ranged from 4,450 to 5,302 cal/g. By applying linear regression analysis to the

experimental data, equations (6) to (11) were obtained to describe the affecting independent variable for each dependent variable, %MY, %MC, %VM, %AC, %FC and HV.

$$MY(\%) = 163.039 - 0.360X_1 - 0.243X_2 + 0.136X_3 + 0.175X_4 - 0.057X_5 \quad (6)$$

$$MC(\%) = 0.404 + 8.040\times10^{-4}X_1 + 6.532\times10^{-5}X_2 + 8.739\times10^{-3}X_3 + 5.051\times10^{-3}X_4 + 0.012X_5 \quad (7)$$

$$VM(\%) = 116.615 - 0.171X_1 - 0.230X_2 + 0.080X_3 - 0.032X_4 + 0.199X_5 \quad (8)$$

$$AC(\%) = -0.929 + 0.028X_1 + 0.032X_2 - 0.044X_3 - 0.044X_4 - 0.035X_5 \quad (9)$$

$$FC(\%) = -16.090 + 0.141X_1 + 0.199X_2 - 0.045X_3 + 0.072X_4 - 0.175X_5 \quad (10)$$

$$HV(cal/g) = 3{,}654.277 + 4.157X_1 - 4.248X_2 + 4.925X_3 + 2.940X_4 + 4.104X_5 \quad (11)$$

The ANOVA test was applied to check the adequacy and reliability of the mathematical model (Yu et al., 2019) based upon the F-test, p-value and coefficient of determination (R^2). The ANOVA results are shown in Table 3. The F-test was used to statistically analyse the experimental data of all responses. The F values for %MY, %MC, %VM, %AC, %FC and HV were 1295.56, 7.77, 65.84, 57.76, 43.01 and 5.72, respectively. The generated models were, therefore, significant. Also, the p-value for all models of responses were <0.05, demonstrating that the obtained models were sufficiently significant to explain the experimental data (Tan et al., 2017). The significance of individual model terms were as follows. X_1, X_2, X_3 and X_4 were found to be significant model for %MY and %AC; X_3 and X_4 were significant model terms for %MC; and X_1 and X_2 were significant model terms for %VM, %FC and HV model. The good fir of the experimental data to the linear model equation was indicated by high R2 values ($R^2_{\%MY}$ = 0.9991, $R^2_{\%MC}$ = 0.8662, $R^2_{\%VM}$ = 0.9821, $R^2_{\%AC}$ = 0.9796, $R^2_{\%FC}$ = 0.9729 and R^2_{HV} = 0.8265). Therefore, the obtained mathematical model of %MY, %MC, %VM, %AC, %FC and HV were predicted to be significant. The adequate precision of all responses, which is the signal to noise ratio, were found higher than 4, indicating that obtained model can be applied for design space navigation (Soleimanzadeh et al., 2019).

The analysis of equation coefficients of the five parameters showed that temperature had a positive effect on %MC, %AC, %FC and HV but a negative effect on %MY and %VC. Time showed a positive effect on %MC, %AC and %FC but a negative effect on %MY, %VC and HV. The effect of oxygen feed was positive on %MY, %MC, %VC and HV but negative on %AC and %FC. The heat rate factor was positive on %MY, %MC, %FC and HV but negative on %VC and %AC. The %MC, %VC and HV received a positive effect from OPF but the effect of OPF was negative for the other responses. The significance order of parameters was determined from the Pareto chart (Figure 2). The upper portion shows the higher effect of variables and then progresses down to the lower effect (Korayem et al., 2015). The results of Pareto analysis show that the most significant independent parameter for %MY, %VC, %AC, %FC and HV was temperature. While the %oxygen was the most significant variable on %MC.

Table 3 ANOVA of the developed model for %MY, %MC, %VC, %AC, %FC and HV

Response	*Source*	*Sum of squares*	*df*	*Mean square*	*F-value*	*p-value*		*Response*	*Source*	*Sum of squares*	*df*	*Mean square*	*F-value*	*p-value*	
%MY	Model	6,042.60	5	1,208.52	1,295.56	< 0.0001	Significant	%AC	Model	47.55	5	9.51	57.76	< 0.0001	Significant
	X_1	5,603.04	1	5,603.04	6,006.58	< 0.0001	Significant		X_1	35.19	1	35.19	213.78	< 0.0001	Significant
	X_2	359.49	1	359.49	385.38	< 0.0001	Significant		X_2	6.10	1	6.10	37.04	0.0009	Significant
	X_3	22.25	1	22.25	23.85	0.0028	Significant		X_3	2.34	1	2.34	14.21	0.0093	Significant
	X_4	57.20	1	57.20	61.32	0.0002	Significant		X_4	3.68	1	3.68	22.33	0.0032	Significant
	X_5	0.6165	1	0.6165	0.6609	0.4473	Non-significant		X_5	0.2369	1	0.2369	1.44	0.2755	Non-significant
	Residual	5.60	6	0.9328					Residual	0.9878	6	0.1646			
	Cor total	6,048.20	11		Adeq. precision = 85.703, R^2 = 0.9991				Cor total	48.53	11		Adeq. precision = 20.965, R^2 = 0.9796		
%MC	Model	0.1942	5	0.0388	7.77	0.0134	Significant	%FC	Model	1,127.41	5	225.48	43.01	0.0001	Significant
	X_1	0.0279	1	0.0279	5.59	0.0560	Non-significant		X_1	869.38	1	869.38	165.84	< 0.0001	Significant
	X_2	0.0000	1	0.0000	0.0052	0.9449	Non-significant		X_2	239.99	1	239.99	45.78	0.0005	Significant
	X_3	0.0917	1	0.0917	18.33	0.0052	Significant		X_3	2.42	1	2.42	0.4624	0.5219	Non-significant
	X_4	0.0478	1	0.0478	9.57	0.0213	Significant		X_4	9.71	1	9.71	1.85	0.2225	Non-significant
	X_5	0.0267	1	0.0267	5.34	0.0601	Non-significant		X_5	5.91	1	5.91	1.13	0.3290	Non-significant
	Residual	0.0300	6	0.0050					Residual	31.45	6	5.24			
	Cor total	0.2242	11		Adeq. precision = 9.839, R^2 = 0.8662				Cor total	1,158.86	11		Adeq. precision = 17.705, R^2 = 0.9729		
%VC	Model	1,606.41	5	321.28	65.84	< 0.0001	significant	HV	Model	9.047E+05	5	1.809E+05	5.72	0.0278	significant
	X_1	1,266.28	1	1,266.28	259.48	< 0.0001	significant		X_1	7.465E+05	1	7.465E+05	23.59	0.0028	significant
	X_2	322.78	1	322.78	66.14	0.0002	significant		X_2	1.096E+05	1	1.096E+05	3.46	0.1120	significant
	X_3	7.75	1	7.75	1.59	0.2544	Non- significant		X_3	29106.75	1	29,106.75	0.9198	0.3746	Non- significant
	X_4	2.01	1	2.01	0.4114	0.5450	Non- significant		X_4	16206.75	1	16,206.75	0.5122	0.5011	Non- significant
	X_5	7.59	1	7.59	1.56	0.2588	Non- significant		X_5	3234.08	1	3,234.08	0.1022	0.7600	Non- significant
	Residual	29.28	6	4.88					Residual	1.899E+05	6	31,643.53			
	Cor total	1,635.69	11		Adeq. precision = 21.840, R^2 = 0.9821				Cor total	1.095E+06	11		Adeq. precision = 6.269, R^2 = 0.8265		

Figure 2 Pareto chart showed the effect of each parameter on (a) %MY (b) %MC (c) %VC (d) %AC (e) %FC and (f) HV (see online version for colours)

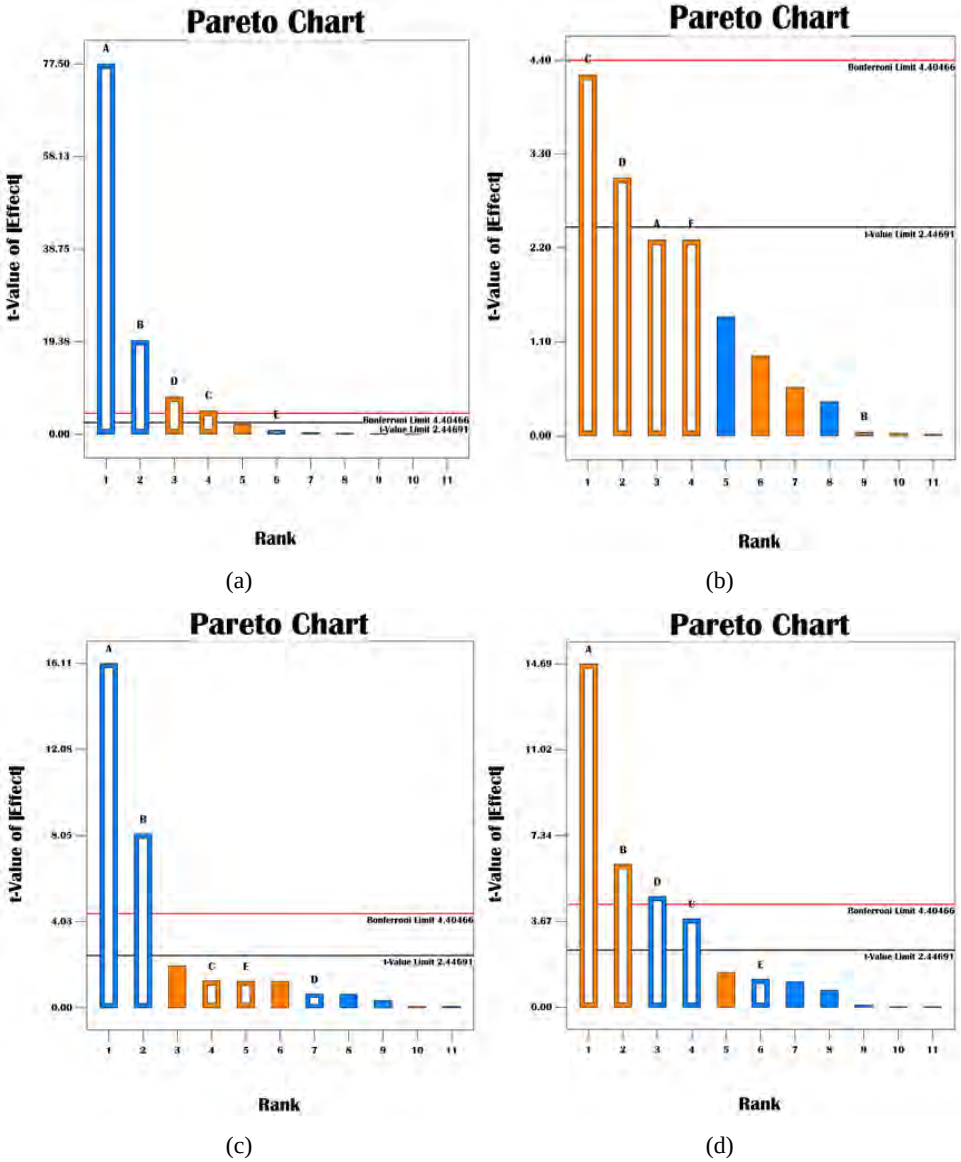

Notes: A = temperature, B = time, C = oxygen feed, D = heat rate, E = OPF size.

Figure 2 Pareto chart showed the effect of each parameter on (a) %MY (b) %MC (c) %VC (d) %AC (e) %FC and (f) HV (continued) (see online version for colours)

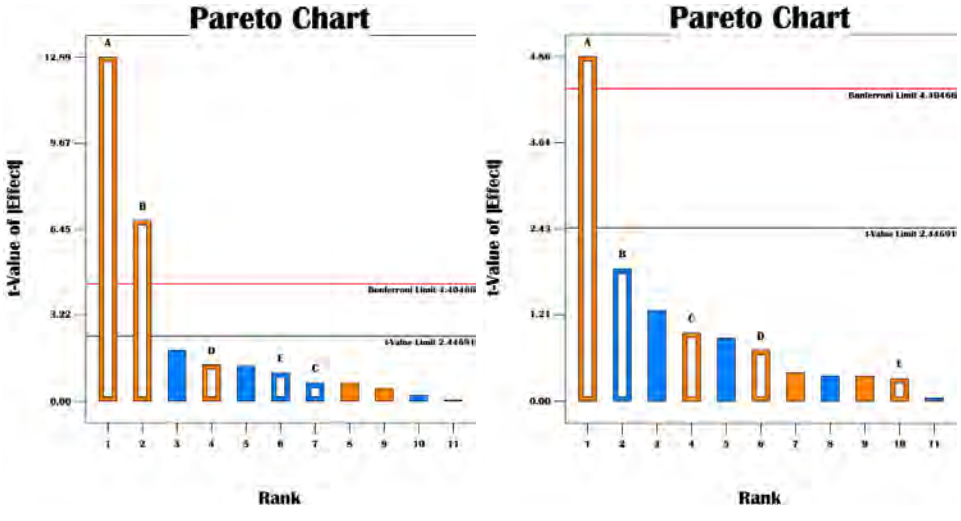

(e) (f)

Notes: A = temperature, B = time, C = oxygen feed, D = heat rate, E = OPF size.

Figure 3 Predicted versus actual diagnostics plots, (a) %MY (b) %MC (c) %VC (d) %AC (e) %FC and (f) HV (see online version for colours)

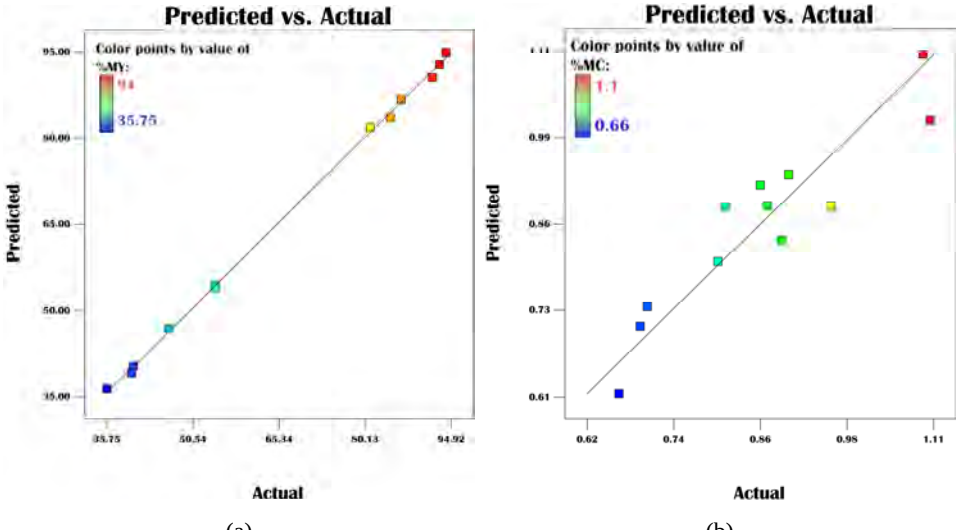

(a) (b)

Figure 3 Predicted versus actual diagnostics plots, (a) %MY (b) %MC (c) %VC (d) %AC (e) %FC and (f) HV (continued) (see online version for colours)

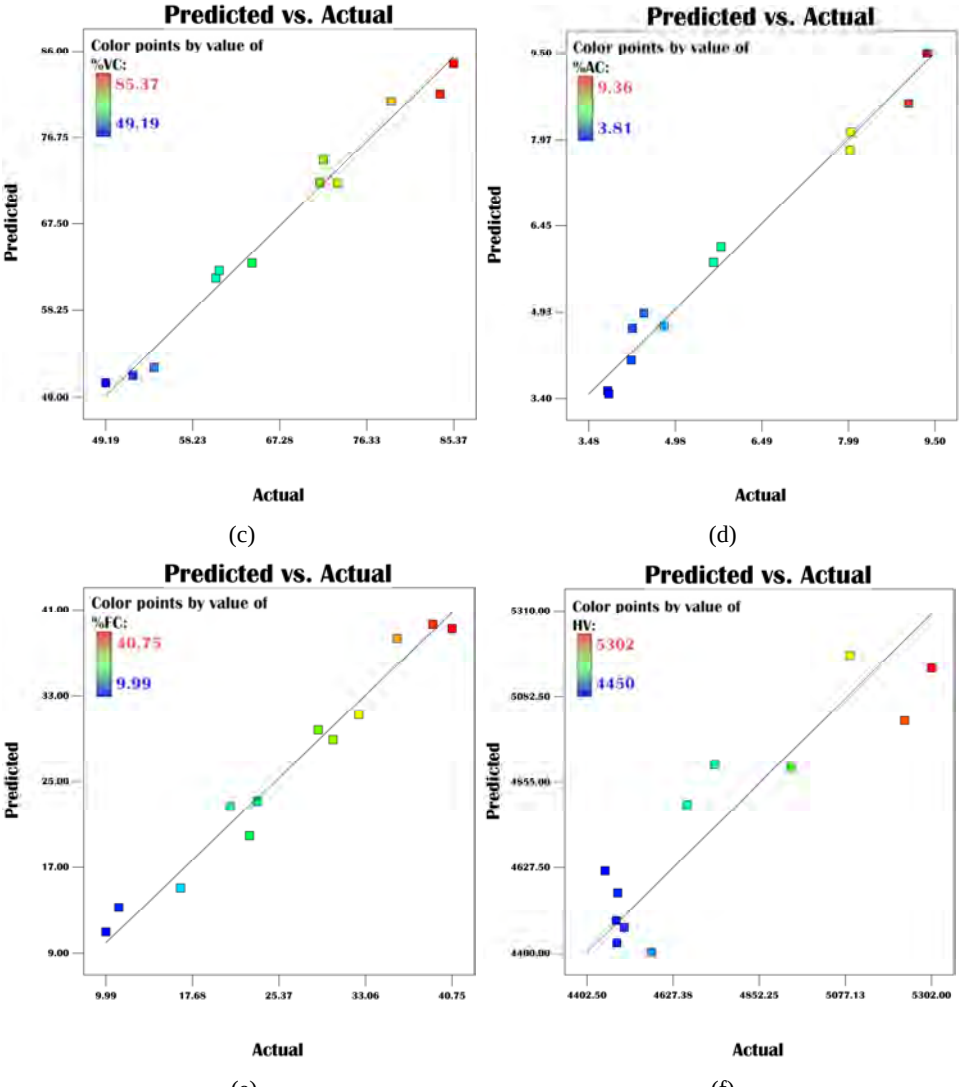

3.2 Diagnostics plot

3.2.1 Predicted versus actual plot

Figures 3(a) to 3(f) show the relationship between predicted values and experimental data. The values of both were quite close and fell on the straight line at an acceptable level. This indicated that the predicted values were in good agreement with the actual

results. It can be concluded from the results that the generated model was significant and adequate for all responses (Bahrami et al., 2018; Ooi et al., 2018).

Figure 4 Normal probability versus internally studentised residuals plots, (a) %MY (b) %MC (c) %VC (d) %AC (e) %FC and (f) HV (see online version for colours)

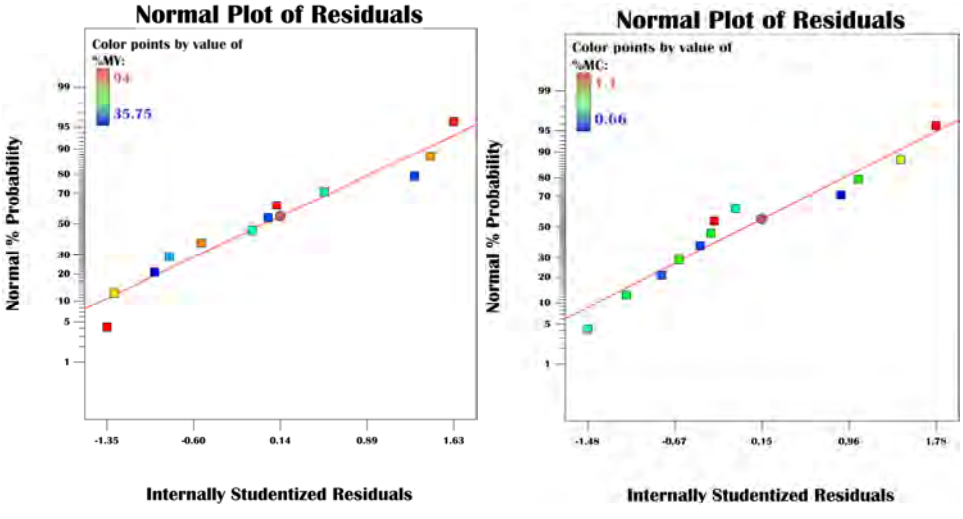

Figure 4 Normal probability versus internally studentised residuals plots, (a) %MY (b) %MC (c) %VC (d) %AC (e) %FC and (f) HV (continued) (see online version for colours)

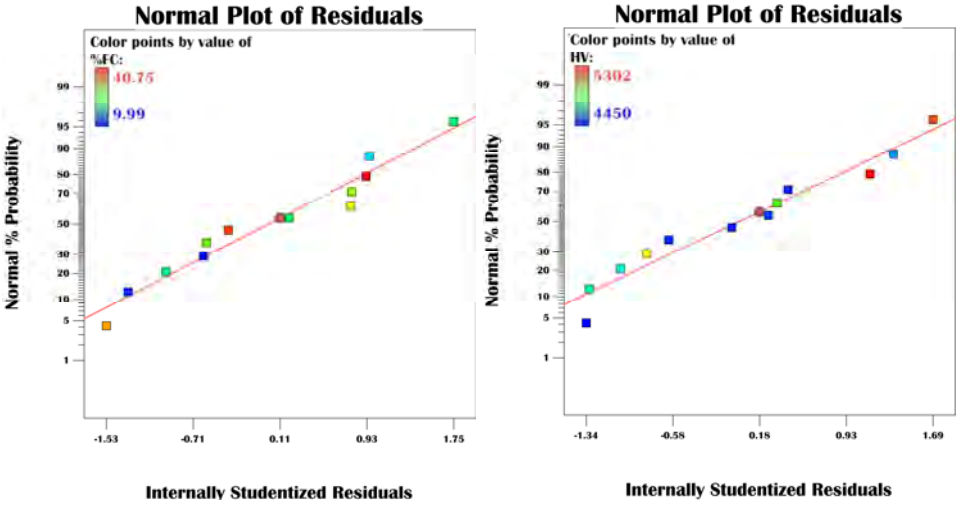

(e) (f)

Figure 5 Internally studentised residual versus predicted value plots, (a) %MY (b) %MC (c) %VC (d) %AC (e) %FC and (f) HV (see online version for colours)

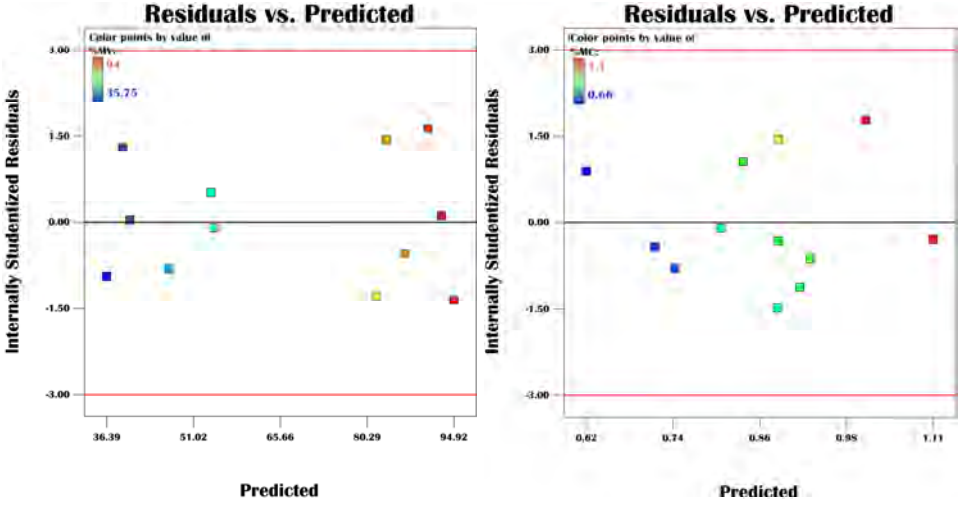

(a) (b)

Figure 5 Internally studentised residual versus predicted value plots, (a) %MY (b) %MC (c) %VC (d) %AC (e) %FC and (f) HV (continued) (see online version for colours)

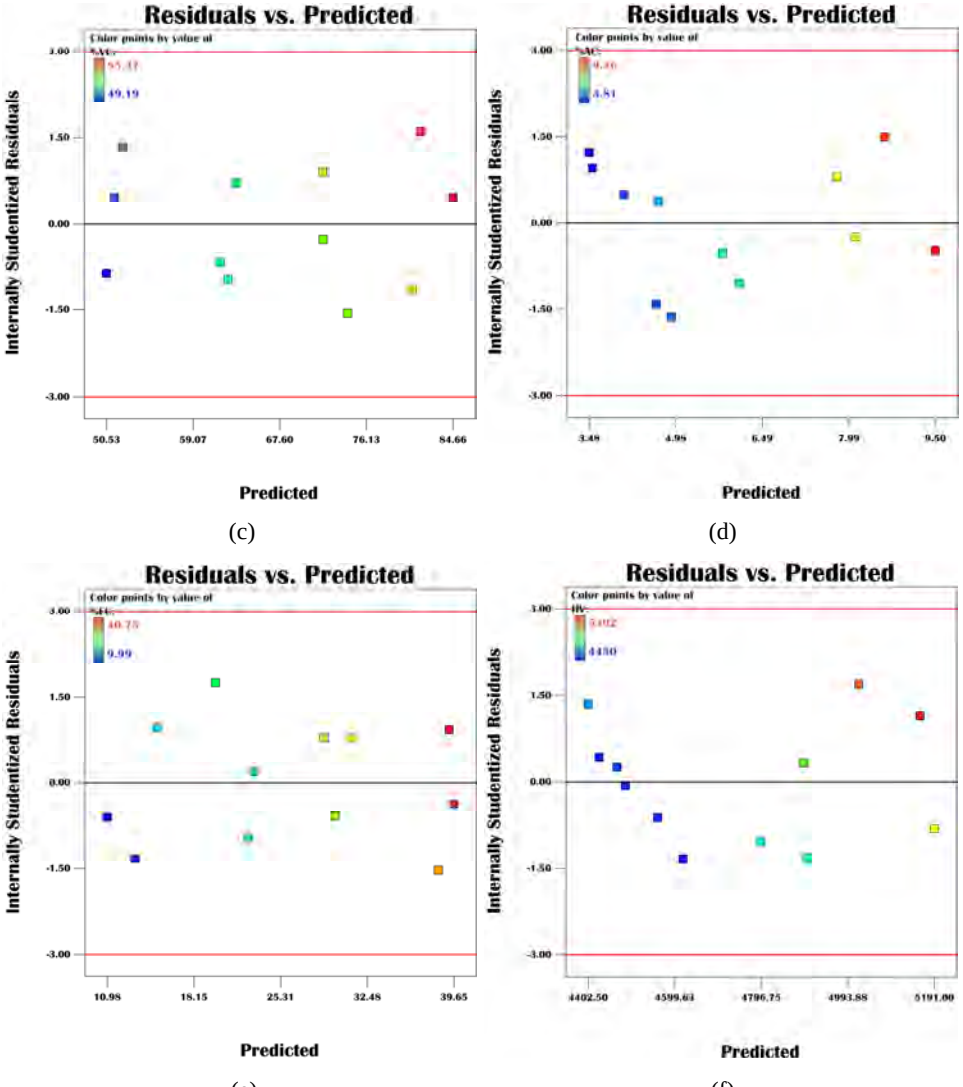

3.2.2 Normal plot of residuals

The plot of normal probability was used to estimate the distribution of the experimental residuals data. The residual plots of six dependent parameters are shown in Figures 4(a) to 4(f). The obtained plots illustrated that most of the data points were fairly close to the diagonal line. The linear behaviour of the residual plots suggest that the normal % probability plot of the experimental residues was normally distributed (Zafar et al., 2018), no large deviation of variance occurred (Sabbagh et al., 2018) and that the response of the mathematic model was, therefore, a good prediction (Hajirahimkhan et al., 2019).

3.2.3 *Internally studentised residual versus predicted value plots*

A plot of internally studentised residuals versus predicted values of the 12 experimental results are shown in Figures 5(a) to 5(f). The random distribution of the experimental data residuals lay between +3 and –3 which is within acceptable limits: the smaller the distribution value of the residual, the more reliable the experimental data. Moreover, the distribution was without any systematic structure. Therefore, the obtained data were reliable and fell within a 95% confidence interval which could be trusted within the ranges studied (Jiang et al., 2019).

Figure 6 Internally studentised residual versus run number plots, (a) %MY (b) %MC (c) %VC (d) %AC (e) %FC and (f) HV (see online version for colours)

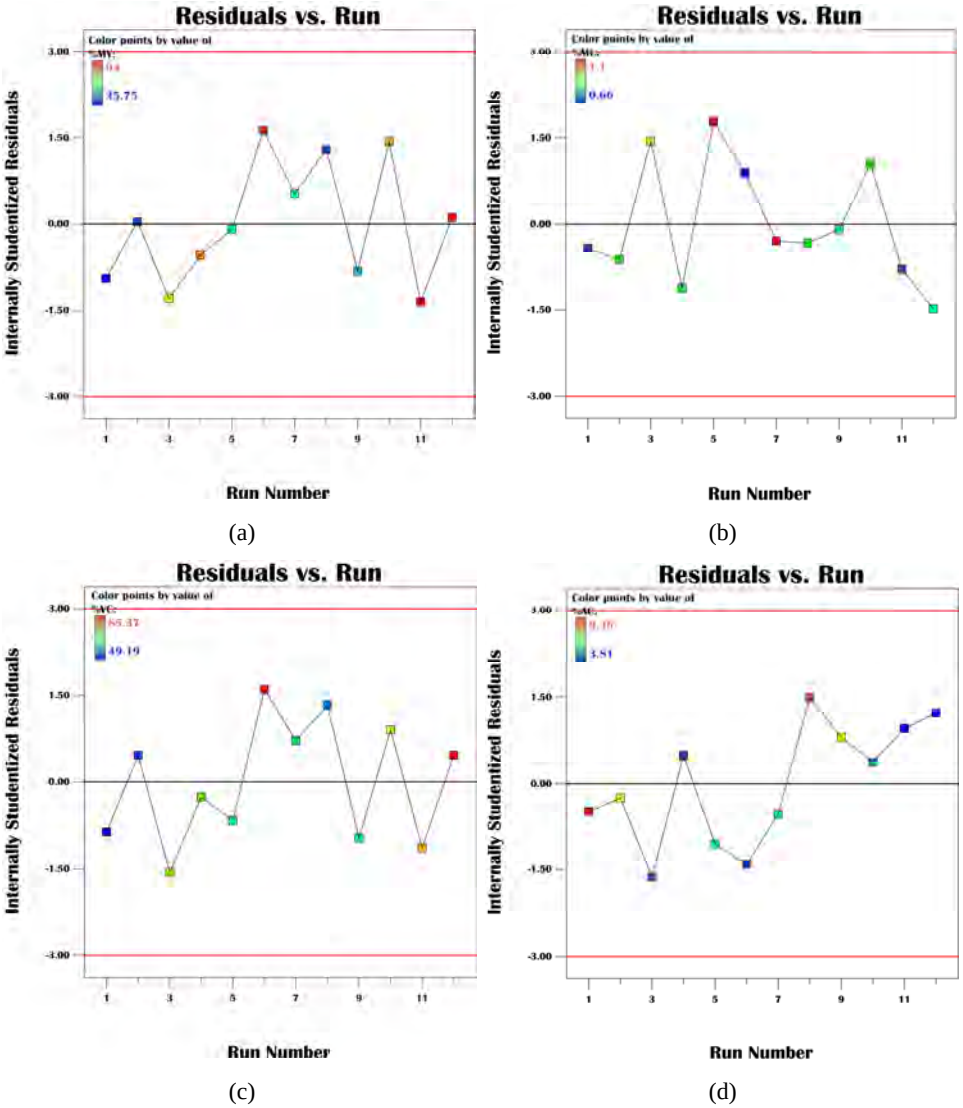

Figure 6 Internally studentised residual versus run number plots, (a) %MY (b) %MC (c) %VC (d) %AC (e) %FC and (f) HV (continued) (see online version for colours)

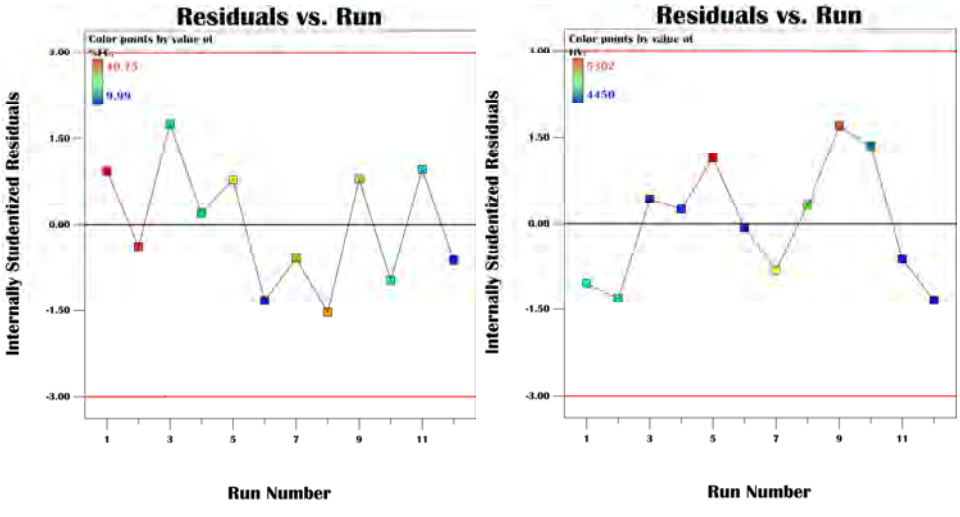

(e) (f)

3.2.4 Internally studentised residual versus run number plots

A plot of internally studentised residuals versus run number of all responses is shown in Figures 6(a) to 6(f). This plot was used to determine the independence of observations (versus order). The plots of residuals in the graphs do not show specific patterns and are dispersed in a random manner. This shows that the observed experimental data for all responses were independent (Masghati and Ghoreishi, 2018).

4 Conclusions

The primary goal of this study was to examine the significant parameters affecting the torrefaction pretreatment of OPF with a view to improving its fuel properties by this process. The ANOVA results showed that temperature, time, %oxygen feed rate and heat rate were the significant factors affecting the treatment process, while OPF size was not significant for any response. The generated model based on the regression equation was in perfect compliance with the experimental results. The diagnostics plot showed the reliability of all responses. Based on the results, %MC and %VC of torrefied OPF were reduced, while %AC, %FC and HV were increased. Therefore, torrefaction is a technique which has the potential to improve the fuel properties of OPF.

Acknowledgements

The authors would like to thank the Nation Research Council of Thailand (NRCT) for financially supported this research. We also thank the Faculty of Engineering, Thaksin University, Phatthalung for the research equipment and facilities provided to conduct our study.

References

Bahrami, H., Eslami, A., Nabizadeh, R., Mohseni-Bandpi, A., Asadi, A. and Sillanpää, M. (2018) 'Degradation of trichloroethylene by sonophotolytic-activated persulfate processes: optimization using response surface methodology', *Journal of Cleaner Production*, Vol. 198, pp.1210–1218, DOI: https://doi.org/10.1016/j.jclepro.2018.07.100.

Campbell, W.A., Coller, A. and Evitts, R.W. (2019) 'Comparing severity of continuous torrefaction for five biomass with a wide range of bulk density and particle size', *Renewable Energy*, Vol. 141, pp.964–972, DOI: https://doi.org/10.1016/j.renene.2019.04.057.

Chen, W-H., Lin, B-J., Colin, B., Chang, J-S., Pétrissans, A., Bi, X. and Pétrissans, M. (2018) 'Hygroscopic transformation of woody biomass torrefaction for carbon storage', *Applied Energy*, Vol. 231, pp.768–776, DOI: https://doi.org/10.1016/j.apenergy.2018.09.135.

Cheng, X., Huang, Z., Wang, Z., Ma, C. and Chen, S. (2019) 'A novel on-site wheat straw pretreatment method: Enclosed torrefaction', *Bioresource Technology*, Vol. 281, pp.48–55, DOI: https://doi.org/10.1016/j.biortech.2019.02.075.

Chiou, B-S., Valenzuela-Medina, D., Bilbao-Sainz, C., Klamczynski, A.K., Avena-Bustillos, R.J., Milczarek, R.R., Du, W-X., Glenn, G.M. and Orts, W.J. (2015) 'Torrefaction of pomaces and nut shells', *Bioresource Technology*, Vol. 177, pp.58–65, DOI: https://doi.org/10.1016/j.biortech.2014.11.071.

Energy, M.o. (2019) 'Biomass', [online] http://biomass.dede.go.th/biomass_web/index.html (accessed 31 May 2019).

Gan, Y.Y., Ong, H.C., Ling, T.C., Chen, W.-H. and Chong, C.T. (2019) 'Torrefaction of de-oiled Jatropha seed kernel biomass for solid fuel production', *Energy*, Vol. 170, pp.367–374, DOI: https://doi.org/10.1016/j.energy.2018.12.026.

Hajirahimkhan, S., Ragogna, P.J. and Xu, C. (2019) 'Methacrylation of kraft lignin for UV-curable coatings: process optimization using response surface methodology', *Biomass and Bioenergy*, Vol. 120, pp.332–338, DOI: https://doi.org/10.1016/j.biombioe.2018.11.038.

Jiang, C., Sun, G., Zhou, Z., Bao, Z., Lang, X., Pang, J., Sun, Q., Li, Y., Zhang, X., Feng, C. and Chen, X. (2019) 'Optimization of the preparation conditions of thermo-sensitive chitosan hydrogel in heterogeneous reaction using response surface methodology', *International Journal of Biological Macromolecules*, Vol. 121, pp.293–300, DOI: https://doi.org/10.1016/j.ijbiomac.2018.09.210.

Korayem, A.S., Abdelhafez, A.A., Zaki, M.M. and Saleh, E.A. (2015) 'Optimization of biosurfactant production by Streptomyces isolated from Egyptian arid soil using Plackett-Burman design', *Annals of Agricultural Sciences*, Vol. 60, pp.209–217, DOI: https://doi.org/10.1016/j.aoas.2015.09.001.

Lee, J-W., Kim, Y-H., Lee, S-M. and Lee, H-W. (2012) 'Optimizing the torrefaction of mixed softwood by response surface methodology for biomass upgrading to high energy density', *Bioresource Technology*, Vol. 116, pp.471–476, DOI: https://doi.org/10.1016/j.biortech.2012.03.122.

Masghati, S. and Ghoreishi, S.M. (2018) 'Supercritical CO_2 extraction of cinnamaldehyde and eugenol from cinnamon bark: optimization of operating conditions via response surface methodology', *The Journal of Supercritical Fluids*, Vol. 140, pp.62–71, DOI: https://doi.org/10.1016/j.supflu.2018.06.002.

Nam, H. and Capareda, S. (2015) 'Experimental investigation of torrefaction of two agricultural wastes of different composition using RSM (response surface methodology)', *Energy*, Vol. 91, pp.507–516, DOI: https://doi.org/10.1016/j.energy.2015.08.064.

Ooi, T.Y., Yong, E.L., Din, M.F.M., Rezania, S., Aminudin, E., Chelliapan, S., Abdul Rahman, A. and Park, J. (2018) 'Optimization of aluminium recovery from water treatment sludge using response surface methodology', *Journal of Environmental Management*, Vol. 228, pp.13–19, DOI: https://doi.org/10.1016/j.jenvman.2018.09.008.

Petchseechoung, W. (2017) 'Oil palm industry', [online] https://www.krungsri.com/bank/getmedia/ac87c171-db74-442b-ae29-5b69572896ca/IO_Oil_Palm_2017_EN.aspx (accessed 31 May 2019).

Rasid, R.A., Chin, T.M., Ismail, M. and Rahman, N.N.U.A. (2019) 'Effect of torrefaction temperature, residence time and particle size on the properties of torrefied food waste', *Indonesian Journal of Chemistry*, Vol. 19, No. 3, DOI: 10.22146/ijc.39718.

Sabbagh, F., Muhamad, I.I., Nazari, Z., Mobini, P. and Taraghdari, S.B. (2018) 'From formulation of acrylamide-based hydrogels to their optimization for drug release using response surface methodology', *Materials Science and Engineering: C*, Vol. 92, pp.20–25, DOI: https://doi.org/10.1016/j.msec.2018.06.022.

Singh, R.k., Sarkar, A. and Chakraborty, J.P. (2019) 'Effect of torrefaction on the physicochemical properties of pigeon pea stalk (*Cajanus cajan*) and estimation of kinetic parameters', *Renewable Energy*, Vol. 138, pp.805–819, DOI: https://doi.org/10.1016/j.renene.2019.02.022.

Soleimanzadeh, H., Niaei, A., Salari, D., Tarjomannejad, A., Penner, S., Grünbacher, M., Hosseini, S.A. and Mousavi, S.M. (2019) 'Modeling and optimization of V_2O_5/TiO_2 nanocatalysts for NH3-Selective catalytic reduction (SCR) of NOx by RSM and ANN techniques', *Journal of Environmental Management*, Vol. 238, pp.360–367, DOI: https://doi.org/10.1016/j.jenvman.2019.03.018.

Su, Y., Zhang, S., Liu, L., Xu, D. and Xiong, Y. (2018) 'Investigation of representative components of flue gas used as torrefaction pretreatment atmosphere and its effects on fast pyrolysis behaviors', *Bioresource Technology*, Vol. 267, pp.584–590, DOI: https://doi.org/10.1016/j.biortech.2018.07.078.

Talero, G., Rincón, S. and Gómez, A. (2019) 'Biomass torrefaction in a standard retort: a study on oil palm solid residues', *Fuel*, Vol. 244, pp.366–378, DOI: https://doi.org/10.1016/j.fuel.2019.02.008.

Tan, Y.H., Abdullah, M.O., Nolasco-Hipolito, C. and Ahmad Zauzi, N.S. (2017) 'Application of RSM and Taguchi methods for optimizing the transesterification of waste cooking oil catalyzed by solid ostrich and chicken-eggshell derived CaO', *Renewable Energy*, Vol. 114, pp.437–447, DOI: https://doi.org/10.1016/j.renene.2017.07.024.

Uemura, Y., Omar, W., Othman, N.A., Yusup, S. and Tsutsui, T. (2013) 'Torrefaction of oil palm EFB in the presence of oxygen', *Fuel*, Vol. 103, pp.156–160, DOI: https://doi.org/10.1016/j.fuel.2011.11.018.

Uemura, Y., Saadon, S., Osman, N., Mansor, N. and Tanoue, K.-i. (2015). 'Torrefaction of oil palm kernel shell in the presence of oxygen and carbon dioxide', *Fuel*, Vol. 144, pp.171–179, DOI: https://doi.org/10.1016/j.fuel.2014.12.050.

Wang, L., Barta-Rajnai, E., Skreiberg, Ø., Khalil, R., Czégény, Z., Jakab, E., Barta, Z. and Grønli, M. (2018) 'Effect of torrefaction on physiochemical characteristics and grindability of stem wood, stump and bark', *Applied Energy*, Vol. 227, pp.137–148, DOI: https://doi.org/10.1016/j.apenergy.2017.07.024.

Xu, X., Li, Z. and Jiang, E. (2019) 'Torrefaction performance of camellia shell under pyrolysis gas atmosphere', *Bioresource Technology*, Vol. 284, pp.178–187, DOI: https://doi.org/10.1016/j.biortech.2019.03.091.

Yu, C., Cheng, T., Chen, J., Ren, Z. and Zeng, M. (2019) 'Investigation on thermal-hydraulic performance of parallel-flow shell and tube heat exchanger with a new type of anti-vibration baffle and wire coil using RSM method', *International Journal of Thermal Sciences*, Vol. 138, pp.351–366, DOI: https://doi.org/10.1016/j.ijthermalsci.2018.12.035.

Zafar, S.B., Asif, T., Qader, S.A.U. and Aman, A. (2018) 'Enhanced biosynthesis of dextransucrase: a multivariate approach to produce a glucosyltransferase for biocatalysis of sucrose into dextran', *International Journal of Biological Macromolecules*, Vol. 115, pp.776–785, DOI: https://doi.org/10.1016/j.ijbiomac.2018.04.089.

Zhang, C., Wang, C., Cao, G., Chen, W-H. and Ho, S-H. (2019) 'Comparison and characterization of property variation of microalgal biomass with non-oxidative and oxidative torrefaction', *Fuel*, Vol. 246, pp.375–385, DOI: https://doi.org/10.1016/j.fuel.2019.02.139.